Quest Journals
Journal of Research in Environmental and Earth Sciences
Volume 7 ~ Issue 4 (2021) pp: 46-61
ISSN(Online) :2348-2532
www.questjournals.org

Research Paper

Evaluation of hydrocarbon prospect in Lema area, western parts of Sokoto basin, Nigeria, based on analysis of high resolution aeromagnetic data.

Magaji, Y[1]., Sanusi, Y. A[2*].
1. Ministry of Water Resources, Ilorin, Kwara State, Nigeria.
2. Department of Physics, Usmanu Danfodiyo University, P. M. B. 2346, Sokoto, Nigeria.
**Corresponding author, Sanusi, Y. A*

ABSTRACT: *High resolution aeromagnetic data over Lema and its adjoining area, bounded between 4.00° E and 5.00° E and latitudes 12.00° N and 13.00° N, were analyzed for hydrocarbon investigations to infer the presence of subtle structures and estimate the thickness of the sediments in the area. Results obtained using tilt derivative method suggested existence of four linear and curvilinear regional faults and swarms of lineaments oriented along NNE-SSW, NE-SW, NW-SE, ENE-WSW major trends and E-W, NNW-SSE and WNW-ESE minor trends, reflecting that different stress regimes affected the area during the various stages of its evolution. Results obtained using spectral analysis and local wave number methods suggests that the sedimentary thickness ranges from 0.22 – 1.79 km with the south-eastern part being predominantly shallower than the other parts of the area and the deeper parts separated by basement ridges suggesting horst and graben basement configuration for the area. The maximum thickness of sediments within the deeper parts of the area is generally below the minimum requirement for commencement and generation of hydrocarbons, which suggests that the area may not be viable for hydrocarbon investigations.*

KEYWORDS: *Sokoto basin, Spectral analysis, Local wave number, Tilt derivative, Lineaments, Sedimentary thickness.*

Received 26 April, 2021; Revised: 08 May, 2021; Accepted 10 May, 2021

I. INTRODUCTION

The Nigerian economy, which is heavily dependent on petroleum, has recently been faced with many problems due to falling price of petroleum in the global market. Furthermore, the Niger-delta region where the crude oil is being drilled is facing problems of restiveness which caused decline in the output of the drilled crude oil. Hence, there is the need to both diversify the economy and search for crude oil in the other sedimentary basins in the country, which will improve the earnings of the country. The Sokoto basin , which is located in north-western part of Nigeria, is among the five inland basins in the country which is targeted for petroleum search. Prior to meaningful hydrocarbon exploration, preliminary investigations involving determination of subsurface structures, that can serve as hydrocarbon traps, and estimation of the thickness of sediments is necessary prior to drilling to avoid waste of resources. Analysis using gravity and magnetic methods has been employed world-wide for such analysis. These methods are very cost-effective and enable better detection of subtle lineaments and estimation of sedimentary thickness.

Previous studies in the Sokoto basin mostly involve estimation of sedimentary thickness, delineation of subsurface structures and estimation of Curie point depths and heat flow values using low resolution aeromagnetic data. For example, [1], based on Werner deconvolution method, estimated sedimentary thickness ranging from 1.4 to 2.0 km, while [2] and [3], using spectral analysis method, estimated sedimentary thickness ranging between 1.39 – 1.93 km in the basin. Also, [4] estimated sedimentary thickness of 1.4 – 2.7 km using 2D modelling of low resolution aeromagnetic data while [5] estimated sedimentary thickness ranging between 0.77 – 2.3 km around Birnin-Kebbi and its adjoining areas and delineated several subtle lineaments, which could act as structural traps, oriented along different directions. The main purpose of this study is to analyze high resolution aeromagnetic data over Lema and its adjoining areas contained in the western part of Sokoto basin (Fig. 1), with the main aim of delineating subtle structures and estimation of the thickness of sediments in the area to evaluate the hydrocarbon potential of the area.

II. GEOLOGY OF THE AREA

The Sokoto Basin of Nigeria forms the Southeastern sector of the Iullemmeden Basin, one of the young (Mezoic-Tertiary) inland cratonic sedimentary basins of West Africa. The basin is located in the north-western part of Nigeria and predominantly consists of a gently undulating plain with an average elevation varying from 250 – 400 m [6]. The evolution of the basin has been associated with tectonic movements and/or stretching and rifting of a

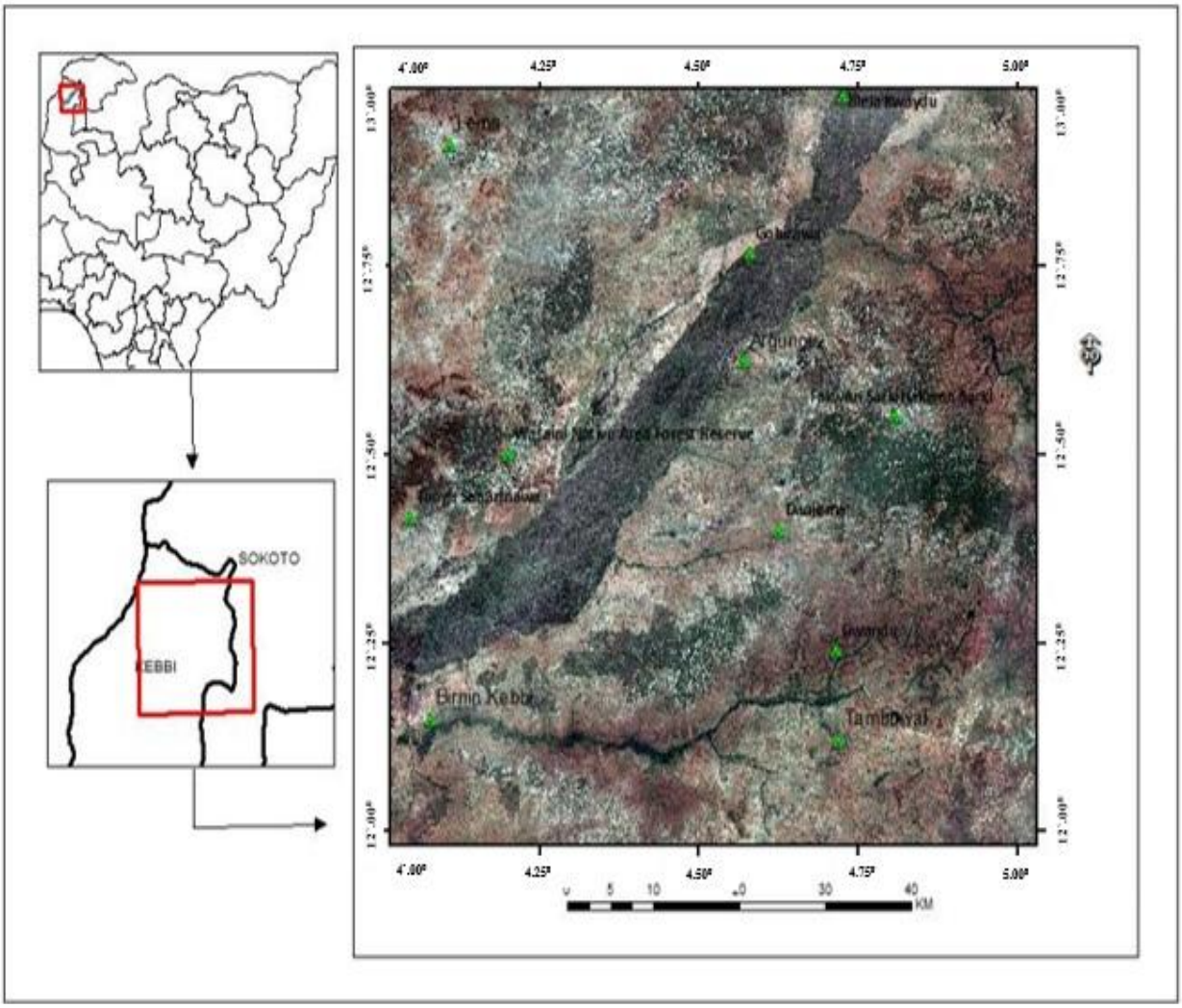

Figure 1: Google Earth map of the study area (Adapted from Google, 2017).

stable tectonic crust in the Palaeozoic [7, 8]. The basin consists of two geologic units, the basement complex and the overlying sedimentary units. The basement complex consists of quartzites and older granite series which intruded the migmatite-gneiss complex and the schist belt. Overlying the basement complex are successions of sedimentary units that were deposited during three main phases of deposition, consisting of two continental phases separated by Maastrichtian – Paleocene marine transgressions.

Sedimentation began in the Pre- Maastrichtian with the deposition of continental deposits consisting of grits and clays of fluviatile and lacustrine origin belonging to Gundumi and Illo Formations unconformably over the basement complex. The two Formations extend northwards into Niger Republic and generally belong to the 'Continental Intercalaire' of West Africa [8]. The Gundumi and Illo Formations were overlain unconformably by the Rima group, containing the Taloka and Wurno Formations and consisting of mudstones and sandstones. The Taloka Formations were separated by shelly and fossiliferous Dukamaje Formation deposited in a marine environment [7]. Subsequently, the Sokoto group consisting of Dange, Kalambaina and Gamba Formations and deposited in a marine environment during the Paleocene era overlies the Rima group, with the Dange and Gamba Formations being separated by the Kalambaina Formation. Finally, the Eocene Gwandu Formation of Tertiary age was deposited over the Sokoto group. The surface geology map (Fig. 2) shows that the predominant

part of the area is covered by the Gwandu Formation except the extreme south-eastern part which is covered by the Wurno Formation.

III. DATA AND METHODS

3.1 Aeromagnetic data

The high resolution total-field magnetic intensity (TMI) digital airborne data used in this study were obtained, at a subsidized price, from the Nigerian Geological Survey Agency (NGSA), Abuja. The digital data covered four half – degree sheets namely; sheet 27 (Lema), sheet 28 (Argungu), sheet 49 (Birnin Kebbi) and sheet 50 (Tambuwal) bounded between longitudes 4.00^0E to 5.00^0E and latitudes 12.00^0 N to 13.00^0 N. The aeromagnetic data were acquired as part of a second nationwide aeromagnetic survey conducted in two phases by Fugro Airborne Surveys between 2005 to 2010 on behalf of the Federal Government of Nigeria (FGN). The data were acquired (i) along a series of NW – SE flight lines at an interval of 500 m, and a tie line spacing of 2000 m along NE- SW direction, (ii) at an average of 80 m terrain clearance, and (iii) data recording interval of 0.1 s (~7 m). The new data has an added advantage of high resolution over the data acquired in the first nationwide survey conducted between 1974 – 1976, which were obtained using a flight elevation of 152 m and flight line spacing of 2000 m.

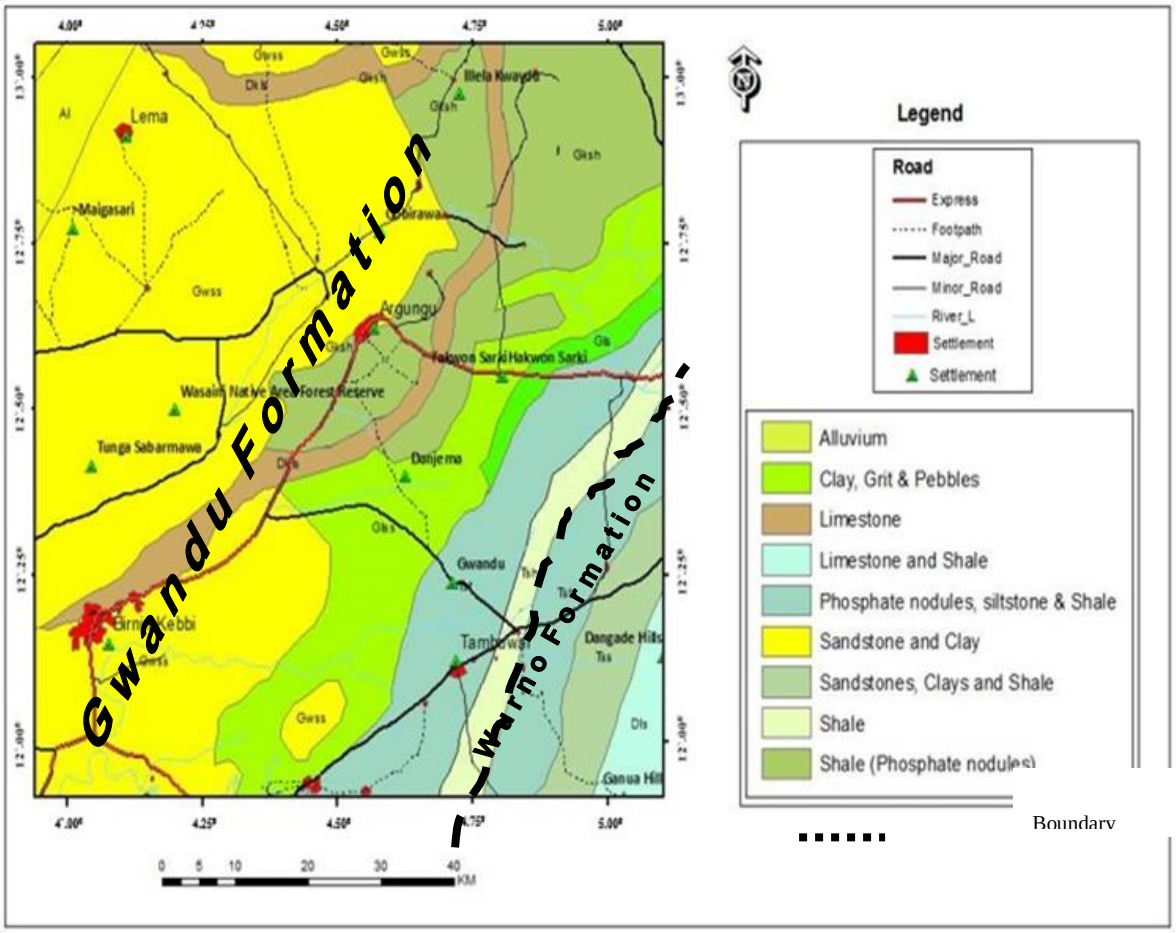

Figure 2: Geologic map of the study area.

3.2 Regional – residual separation and reduction to the equator

The TMI data is composed of regional and residual magnetic field intensity values highlighting the magnetic effects of core, often referred to as the regional field, and that of the crustal rocks, often referred to as the residual field. To estimate the residual magnetic field intensity (RMI) values, which constitute the magnetic effects of subtle crustal rocks, the regional field was modelled as a mathematical plane surface, using multi-regression analysis, and the values were subtracted directly from the TMI values. Further, the RMI values were reduced to the magnetic equator using a phase shift filter known as reduction to equator (RTE) filter to remove the dipolar effects of the magnetic field and align the peaks of the anomalies with the centre of the magnetic sources. The application of RTE filter is considered more appropriate in low latitude regions than the reduction to pole filter which is preferred in high latitude regions [9]. The RTE filter is mathematically expressed as:

$$RTE = \sin I + i \cos I \sin (D - \theta)^2 \quad (1)$$

where I is geomagnetic inclination, D geomagnetic declination, $\sin I$ is the amplitude component, and $i \cos I \sin (D - \theta)^2$ is the phase component. Oasis Montaj (v.6.4.2) software was used for the computation using values of $I = 2.7850$ and D $= -2.0050$ estimated from the IGRF calculator.

The procedure for obtaining the RMI-RTE values involved (i) transforming the RMI values to the frequency domain, using fast Fourier transform (FFT) method [9], (ii) multiplying the Fourier transformed RMI values with the RTE filter in the frequency domain, (iii) inverse Fourier transforming the product obtained back to the space domain to obtain the RMI-RTE values.

3.3 Tilt angle derivative (TDR)

Varieties of methods have been used since 1970's for enhancement of potential field data and detection of subtle lineaments. These methods include those based on vertical derivatives of different orders [9], total horizontal derivatives [10] and ratio of vertical to total horizontal derivatives [11, 12, 13, 14]. The tilt angle derivative (TDR) method which belong to the last mentioned group and has been widely used for subsurface structural mapping is employed in this study. The method is independent of amplitude of the anomaly, shows maxima which peaks over the anomaly and tends to equalize the response from both weak and strong anomalies enabling mapping of shallow and deep-seated structures [11, 12]. The TDR is expressed as [11, 12]:

$$TDR = arctan\left[\frac{\left(\frac{\partial T}{\partial z}\right)}{\left(\frac{\partial T}{\partial h}\right)}\right] \quad (2)$$

Where $$\frac{\partial T}{\partial h} = \left[\left(\frac{\partial T}{\partial x}\right)^2 + \left(\frac{\partial T}{\partial y}\right)^2\right]^{\frac{1}{2}} \quad (3)$$

The sequential steps involved in estimating the TDR filter include (i) transforming the RTE- RMI values from space to frequency domain using fast Fourier transform (FFT), (ii) estimation of the vertical and horizontal derivatives in the frequency domain, (iii) estimation of the TDR filter, using the estimated vertical and horizontal derivatives, as highlighted by equation (2), (iv) multiplication of the transformed RTE-RMI values and the TDR filter in the frequency domain, (v) inverse transforming the product back to the space domain.

The contact locations, whose outline define the outline of the subtle structures, were determined by passing a moving window into the TDR data and for each pass, the data within the window were scanned along the horizontal, vertical and diagonal directions using the maxima tracking algorithm of [15]. The tracked maxima locations which represent the contact bodies are denoted by selected symbols. Finally, the lineaments were inferred from the outline of the delineated contacts.

3.4 Spectral analysis

Magnetic anomalies are caused by magnetic sources buried at different depths in the subsurface. [16] have shown that the power spectrum (PS) due to an ensemble of magnetic sources associated with random magnetization at a given depth (z), and assuming the thickness and size factors are negligible, can be expressed as [17]

$$PS\ (k) = Cexp(-2zk) \quad (4)$$

where k is the wave number expressed in radians/ unit distance C is a constant. Equation (4) can further be expressed as

$$\ln[PS\ (k)] = \ln C - 2zk \quad (5)$$

consequently a plot of natural logarithm of PS against the wave number is expected to give a straight line whose slope can be used to estimate the depth value.

To estimate the power spectrum, the RTE-RMI data were partitioned into sixteen blocks, each of 28 km × 28 km dimension, which were further extended on all sides to minimize edge effects or Gibb's phenomenon [9]. Subsequently, the power spectrum was estimated by (i) transforming the data to the frequency domain using fast Fourier transform (FFT) method, (ii) 2 – D Fourier transforming the data in the frequency domain, and (iii) squaring the Fourier transform and dividing it by the number of points. The estimated power spectrum was further smoothened in a concentric annulus to obtain the radially averaged power spectrum (RAPS) [18]. The logarithm of the RAPS was plotted against the radial frequency (f) for each block and linear segments representing subtle magnetic sources at different depths were obtained. Data points within the linear segments were fitted with a least squares best fitting line whose half slope value is equivalent to the depths to the magnetic sources.

3.5 Local wave number method

The local wave number (LWN) method is one of the semi-automated methods employed in estimating the depth to the top of magnetic sources using the complex attributes of analytical signal of the magnetic field

[17, 19, 20] and can be applied to both profile and gridded data. The method uses a local wave number term, which requires both the first and second derivatives of the anomaly field for its estimation. It is mathematically expressed for a gridded data as [21]

$$K(x,y) = \frac{1}{\left(\frac{\partial^2 T}{\partial x^2}+\frac{\partial^2 T}{\partial y^2}+\frac{\partial^2 T}{\partial z^2}\right)^2}\left(\frac{\partial^2 T}{\partial x \partial y}\frac{\partial T}{\partial x}+\frac{\partial^2 T}{\partial y \partial z}\frac{\partial T}{\partial y}+\frac{\partial^2 T}{\partial z^2}\frac{\partial T}{\partial z}\right) \quad (6)$$

Where $\frac{\partial T}{\partial x}, \frac{\partial T}{\partial y}, \frac{\partial T}{\partial z}$ are the derivatives of the total-field magnetic intensity along x, y and z directions respectively. Further, the local wavenumber is related to the structural index (SI), the depth to the top of isolated linear geologic sources (Z_0) and the horizontal distance to the causative source in the form [21, 22]

$$K(x,y) = \frac{(SI+1)Z_0}{h^2+{Z_0}^2} \quad (7)$$

For contact bodies SI = 0 and at the maximum h = 0, hence

$$Z_0 = \frac{1}{k(x,y)} \quad (8)$$

The implementation of the local wave number method in this study began with the estimation of the horizontal and vertical derivatives of the RTE-RMI values in the frequency domain using the FFT method. The values of the derivatives were then used to generate the local wavenumber grid, as suggested by equation (6). The local wave number grid was subsequently scanned using a 3 x 3 moving data window along horizontal, vertical and diagonal directions, using the maxima tracking algorithm of [15], to determine the contact locations. The outline of the contact locations were then used to estimate the depth to the top of the contact locations using the curve-fitting method of [21].

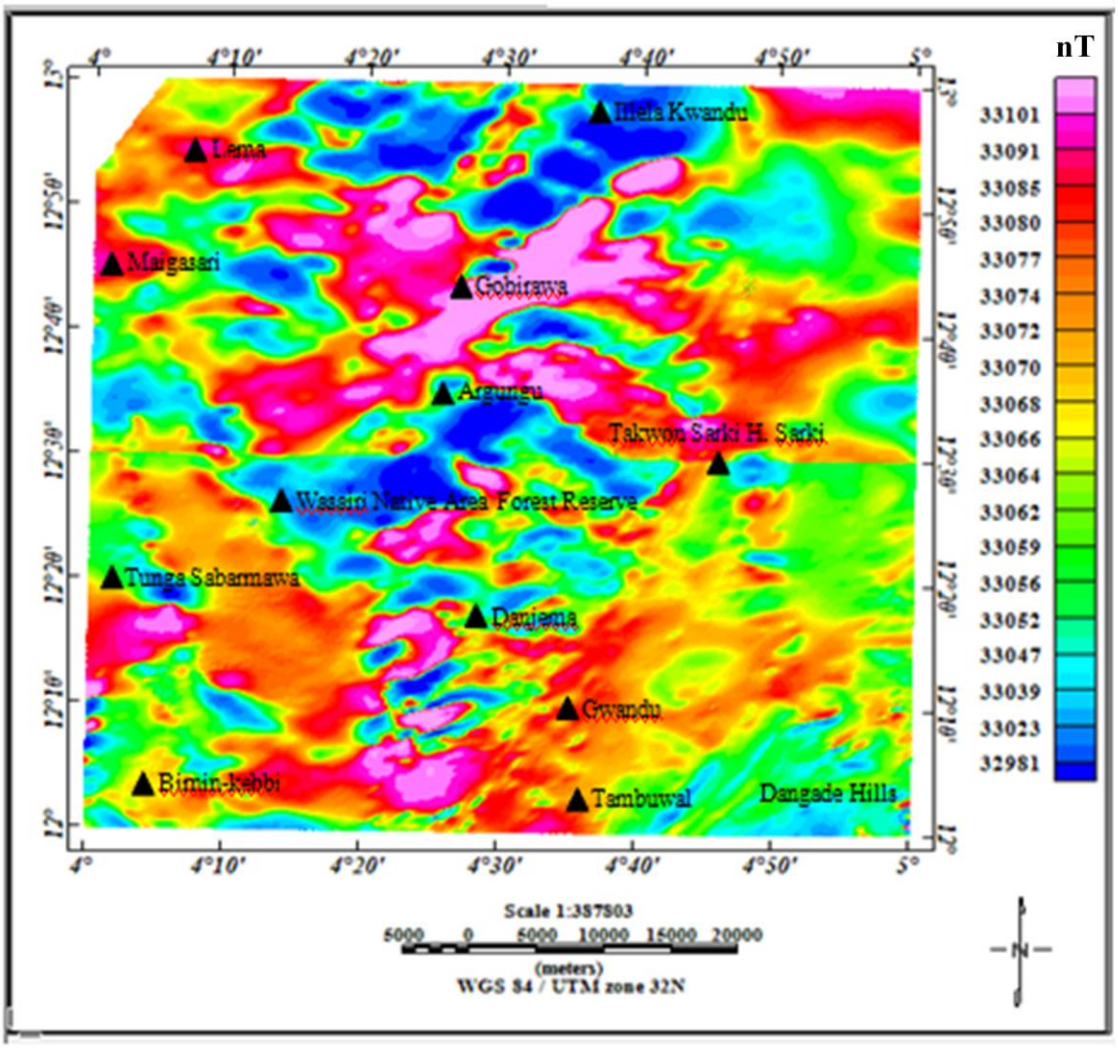

Figure. 3: Total-field magnetic intensity (TMI) map of the study area.

IV. RESULTS AND DISCUSSION

The total-field magnetic intensity (TMI) map (Fig. 3) shows three main types of total-field magnetic anomalies ranging in intensity from 32981– 33101nT. The anomalies were classified into high, moderate and low amplitude anomalies. The high amplitude TMI associated with intensity between 33070 to 33101 nT, and depicted in red and pink colours, occupied (i) predominant portion of the northern central part, around Gobirawa, (ii) central and south-central part of the study area, (iii) north-western part around Lema, and (iv) extreme south-western part around Tunga Sabarmawa. Both the moderate amplitude TMI anomalies with values ranging from 33064 to 33070 nT, shown in yellow and green colours and the low amplitude TMI anomalies ranging in intensity from 32981 to 33064 nT and depicted in blue colour are widespread throughout the study area. Generally, the anomalies were depicted in form of short and long wavelength anomalies which are linear and circular in shape trending along ENE-WSW, NE- SW, E-W and NW- SE directions.

The colour shaded map of the RMI-RTE map (Fig. 4) shows short and long wavelength negative and positive anomalies associated with values ranging from -66.8 to 37.5 nT, depicting lateral variation in the magnetite contents of the subtle crustal rocks beneath the area. In this map, the peaks of the anomalies have been aligned with the centre of the magnetic sources. High positive anomalies, reflecting lithologies of low magnetic susceptibility contrasts such as felsic rocks, predominantly occupies the extreme north-eastern and north-western, north-central and south-central parts while the negative anomalies, reflecting lithologies of high magnetic susceptibility contrasts such as mafic to ultra-mafic rocks , are wide-spread in the study area. In contrast to high latitude regions, high positive anomalies reflect magnetic sources of low susceptibilities and vice versa in low latitude regions [23, 24]. The anomalies are aligned along NE-SW, ENE-WSW, NW-SE, E-W directions suggesting that the area has been affected by Late Pan-African and Pre-Pan African tectonics. Generally, the anomalies are circular and linear in shape.

The TDR map (Fig. 5) is characterized by anomalies that are circular and elliptical in shape, ranging in amplitude from -1.35 to 1.29 nT/m. Both the positive and negative anomalies are wide-spread in the study area, and are linear and circular in shape, trending along The TDR map (Fig. 5) is characterized by anomalies that are circular and elliptical in shape, ranging in amplitude from -1.35 to 1.29 nT/m. Both the positive and negative anomalies which are linear and circular in shape, are wide-spread in the study area, and trending along NE-SW, ENE-WSW, NW-SE, E-W directions. Generally, positive TDR anomalies reflect position of magnetic sources while negative values reflect positions away from magnetic sources [14]. Superposed on the TDR map are the inferred linear and curve linear lineaments, interpreted as major and minor faults in the area. Comparison between Fig. 5 and Figs. 3

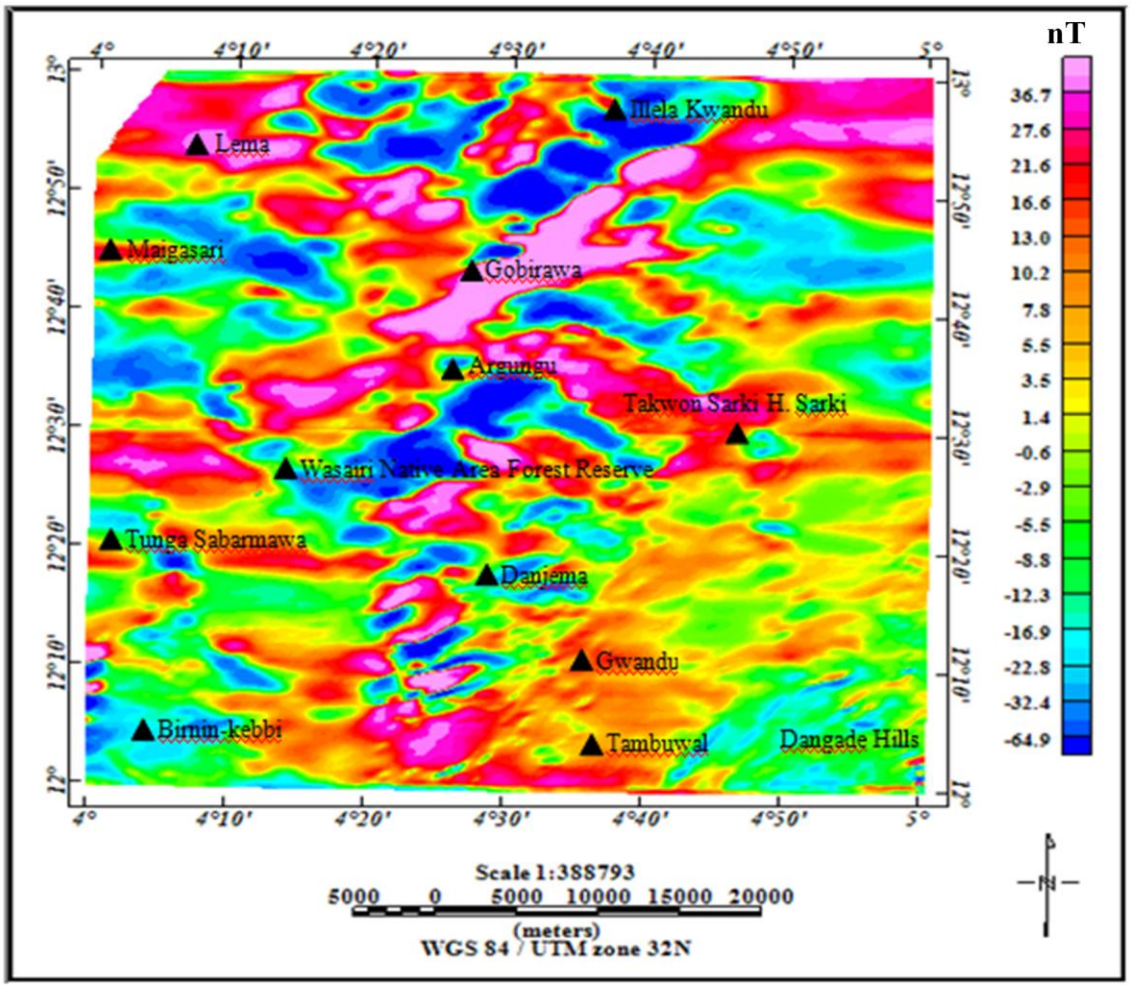

Figure 4. Reduced to equator residual magnetic field intensity (RTE-RMI) map of the study area.

and 4 shows that (i) the edges of the TDR anomalies are sharper than those of the TMI and RTE-RMI anomalies and (ii) the trends of the TDR anomalies are consistent with the trends of the TMI and RTE-RMI anomalies.

The inferred structural map of the area (Fig. 6) shows four NE – SW trending major faults AA', BB', CC' and DD', and swarms of minor faults in-between the major faults trending in different directions. Among these lineaments, AA' and BB' which apparently cross the study area could serve as migrational pathways for hydrocarbons and hydrothermal fluids [25], while CC' and DD', which are curve-linear in shape and restricted within the study area, could serve as structural traps for hydrocarbons and hydrothermal fluids. Among the major lineaments, AA' and BB' were earlier mapped in the area [1,7] from which BB' was linked with the Touside fault identified in the Tibesti region within the Pelusium megashear system [26]. The rest of the major lineaments reflect hitherto unmapped major lineaments in the area. It is pertinent to mention that the inferred structural set up of the study area mimics that of Middle Benue Trough and Bornu basin [25, 27] which is interpreted to suggest that the stress regime associated with the Santonian deformation that was responsible for the tectonic events beneath the Benue Trough and the Bornu basin, which caused the reactivation of the Pan-African lineaments [28], has extended into the Sokoto basin or similar tectonic events contemporaneous with the Santonian deformation in the Benue and Bornu basis has occurred in the Sokoto basin within the various stages of its development.

Result of the statistical analysis of the orientations of the inferred lineaments (Fig. 7) shows NNE-SSW, NE-SW, NW-SE, ENE-WSW major trends and E-W, NNW-SSE and WNW-ESE minor trends. The various trends of the lineaments suggest that different stress regimes along different orientations affected the area and perhaps the entire Sokoto basin, during the various stages of its evolution. The major trends are consistent with the trends of the Pan- African lineaments (600 ± 200 Ma) [29, 30, 31], linked with the Pan – African event attributed to the break-up between the African and South American Continents, and later reactivated as sinistral strike-slip faults in the Early Cretaceous due to convergence of African and South American plates [32]. On the other hand, the minor lineaments were interpreted to be linked with the Kibaran

(1100 ± 200 Ma) and Liberian (2500 ± 200 Ma) orogenies associated with the Pre- Pan- African event [33, 34], and later reactivated in response to tectonic pulses of the post- Cretaceous era associated with (i) major changes in the direction of plate convergence between the African, Arabian plate and the Eurasian plate, and (ii) northerly convergence of the African plate with the Anatolian plate. The lineament trends identified in this study are consistent with the (i) ENE-WSW, NE-SW, E-W, NW-SE, NNE-SSW, and NNW- SSE trends, identified using low resolution aeromagnetic data [5], (ii) ENE-WSW, NE-SW, E- W, and NW-SE trends, identified using landsat imagery [35], and (iii) NE-SW, NW-SE, NNE-SSW and WNW- ESE trends identified using gravity data in the area [36].

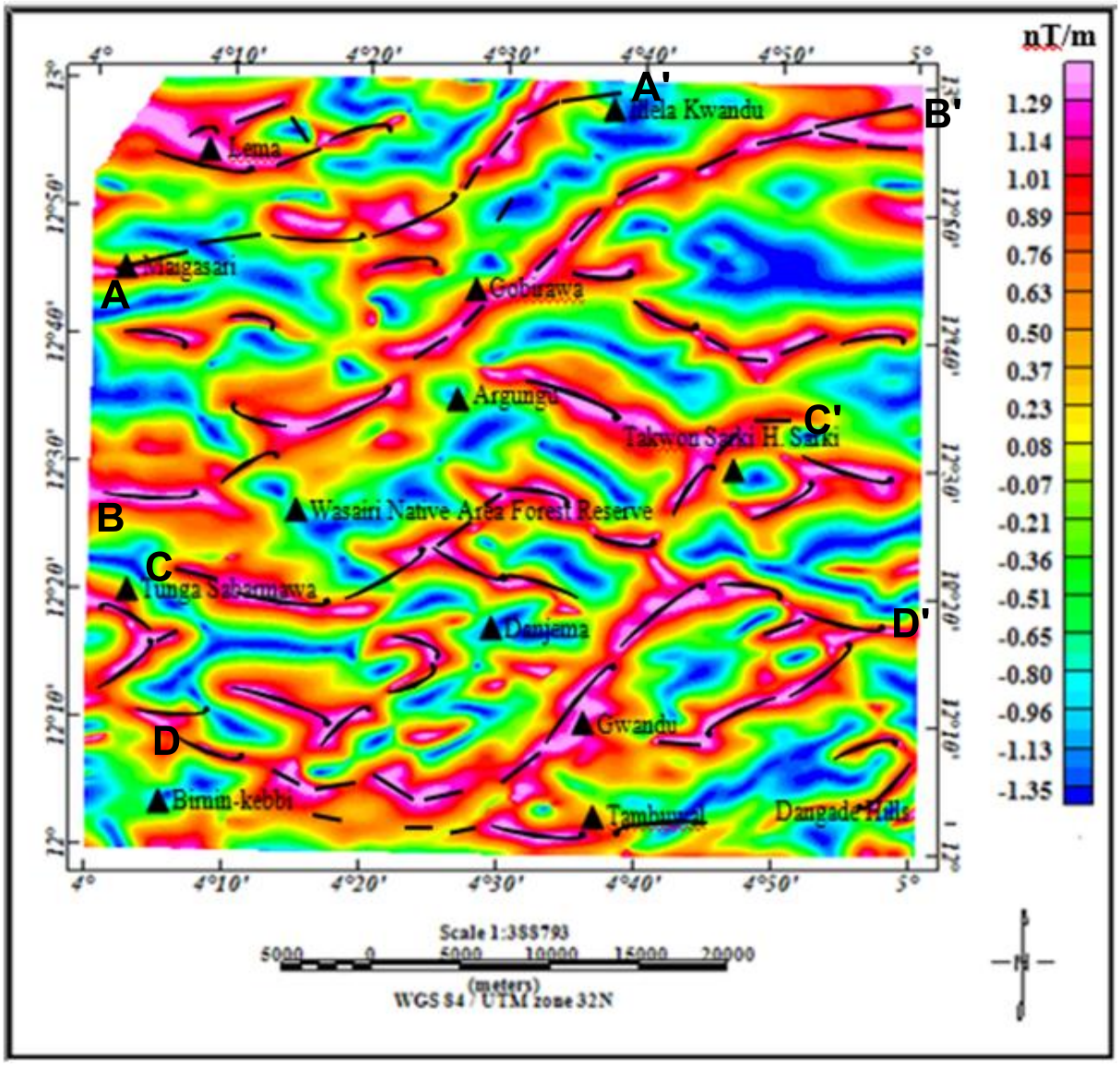

Figure 5: Tilt derivative map of the study area. Superposed on the map are the outlines of the inferred contact bodies.

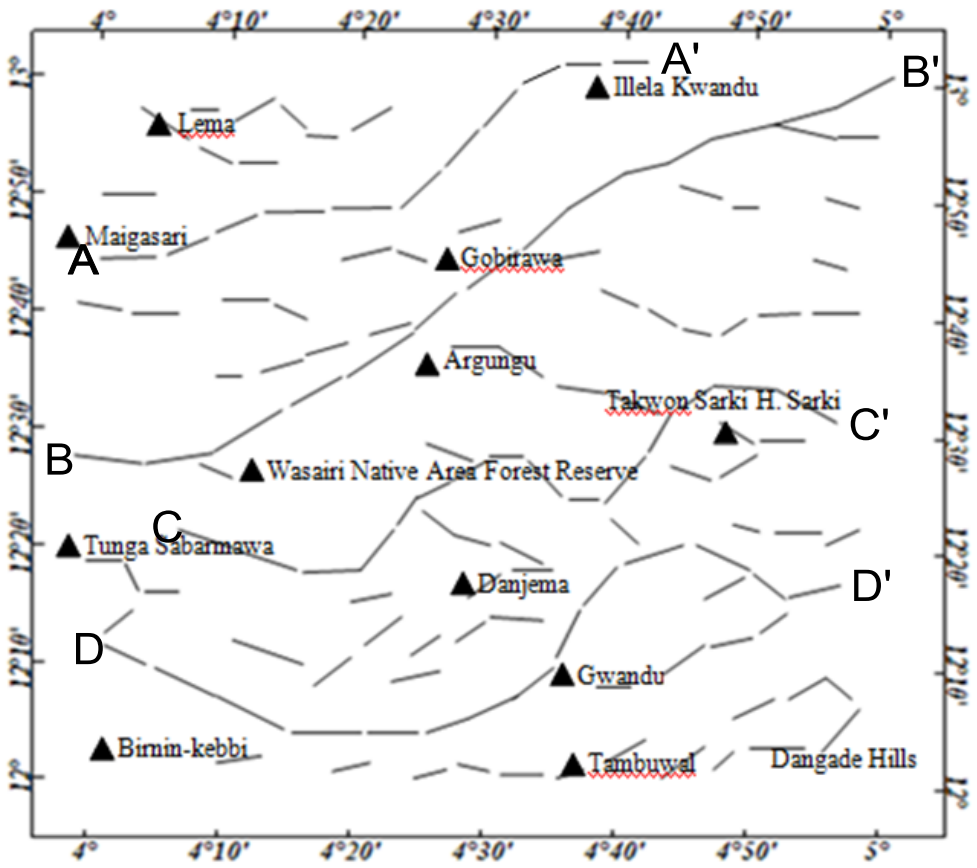

Figure 6. Structural map of the area inferred from the TDR map of the study area.

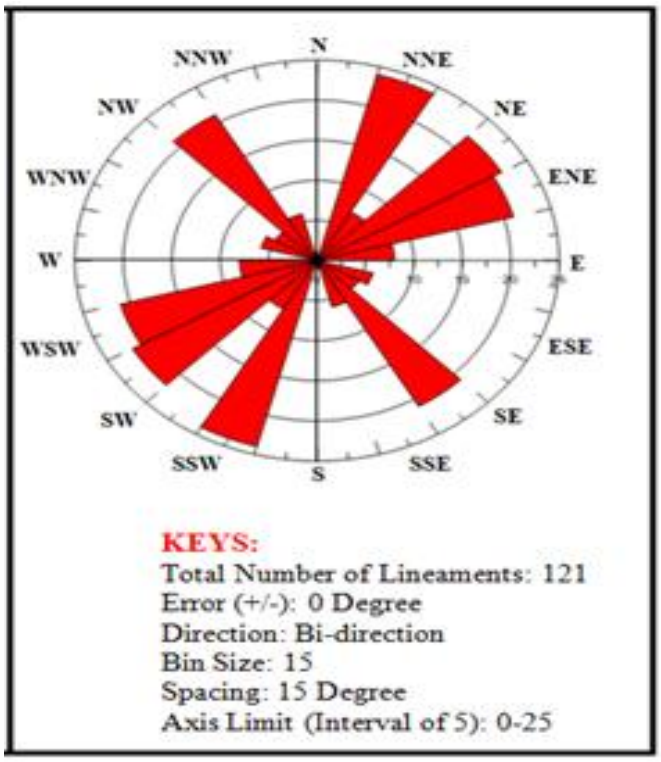

Figure 7: Rose diagram showing the different orientations of the inferred lineaments.

Figure 8 shows typical plots of natural logarithm of the RAPS against frequency for block 14. The plots show decay in the power spectra with increasing frequency. Rapid decay of the spectra, highlighting steep gradient, was observed in the low wave number component and a steady decay, highlighting a gentle gradient, in the high wave number component. This trend was observed to be consistent with all the other plots of the remaining blocks analyzed. Further, the power spectra associated with the low wave number component were interpreted to reflect contributions from the deeper magnetic sources while the high wave number component emanate from the shallow magnetic sources. Table 1 shows the depths associated with the deep and shallow sources for all the twenty-five blocks analyzed. Z_1 represents depth to deeper magnetic sources which vary from 0.83 km to1.95 km with an average value of 1.40 km, while Z_2 represents depths to shallow magnetic sources, attributed to the magnetic rocks that intrude the sedimentary formation, varying from 0.23 km to 0.79 km with an average value of 0.47 km.

Figure 9 shows that the depth to shallow magnetic sources beneath the area ranges from 0.29 to 0.67 km. The minimum depth was found around Tambawal in the south-eastern part and around Argungu in the central part of the area while the maximum depth was found north of Lema, in the north-western part, and west of Gwandu in the south-western part. The depth range is consistent with that obtained (0.31 – 0.56 km) in south-eastern part of Sokoto basin [37] and fairly consistent with that obtained (0.22 – 0.96 km) in the lower Sokoto basin [3]

Figure 10 shows the map of the depths to deeper magnetic sources highlighting the undulations of the basement topography beneath the study area. Regions of basement uplift are apparent in the central and lower southern half and are marked by anomalies A, B, C, and D with depths between 0.83 – 1.2 km. The trend of these anomalies are E – W for anomalies A, B, D and NE-SW for anomaly C. Also, deeper areas associated with thick sediments of thickness between 1.7 - 1.95 km, interpreted as sub basins and depicted as anomalies E, F, G and H, were observed in the top northern around Lema and Illela Gwandu, east-central around Takwon Sarki, and west-central parts around Tunga Sabarmawa. Anomalies E, F and H trend along E-W direction while G trends along NE-SW direction. Sub basins H and E, and H and G are separated by basement uplifted regions, suggesting horst and graben basement configuration for the area. It is worth mentioning that the sedimentary thickness obtained is consistent with the previous estimates in the study area and Sokoto basin in general [1, 3, 4, 37, 38].

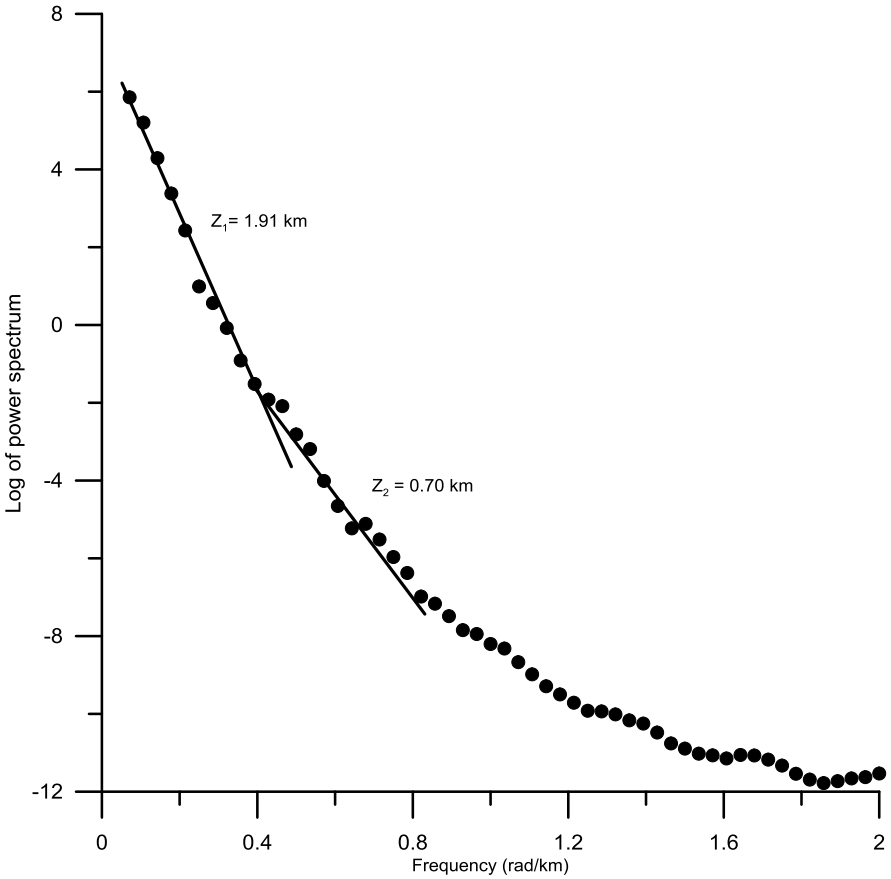

Figure 8. Example of the radially averaged power spectrum for block 14 with two linear segments representing depths of 1.91 and 0.70 km respectively.

Table 1. Estimated depths obtained from spectral analysis method in the study area.

Block	Longitude	Latitude	Z_1 (Km)	Z_2 (Km)
1	4.1	12.1	1.49	0.38
2	4.3	12.1	0.83	0.61
3	4.5	12.1	0.98	0.61
4	4.7	12.1	1.48	0.28
5	4.9	12.1	0.92	0.43
6	4.1	12.3	1.45	0.33
7	4.3	12.3	1.63	0.79
8	4.5	12.3	1.28	0.62
9	4.7	12.3	1.06	0.23
10	4.9	12.3	1.33	0.35
11	4.1	12.5	1.30	0.41
12	4.3	12.5	1.16	0.38
13	4.5	12.5	0.97	0.24
14	4.7	12.5	1.91	0.70
15	4.9	12.5	1.44	0.40
16	4.1	12.7	1.23	0.37
17	4.3	12.7	1.54	0.42
18	4.5	12.7	1.35	0.31
19	4.7	12.7	1.32	0.65
20	4.9	12.7	1.51	0.31
21	4.1	12.9	1.75	0.67
22	4.3	12.9	1.93	0.74
23	4.5	12.9	1.70	0.54
24	4.7	12.9	1.95	0.55
25	4.9	12.9	1.45	0.38

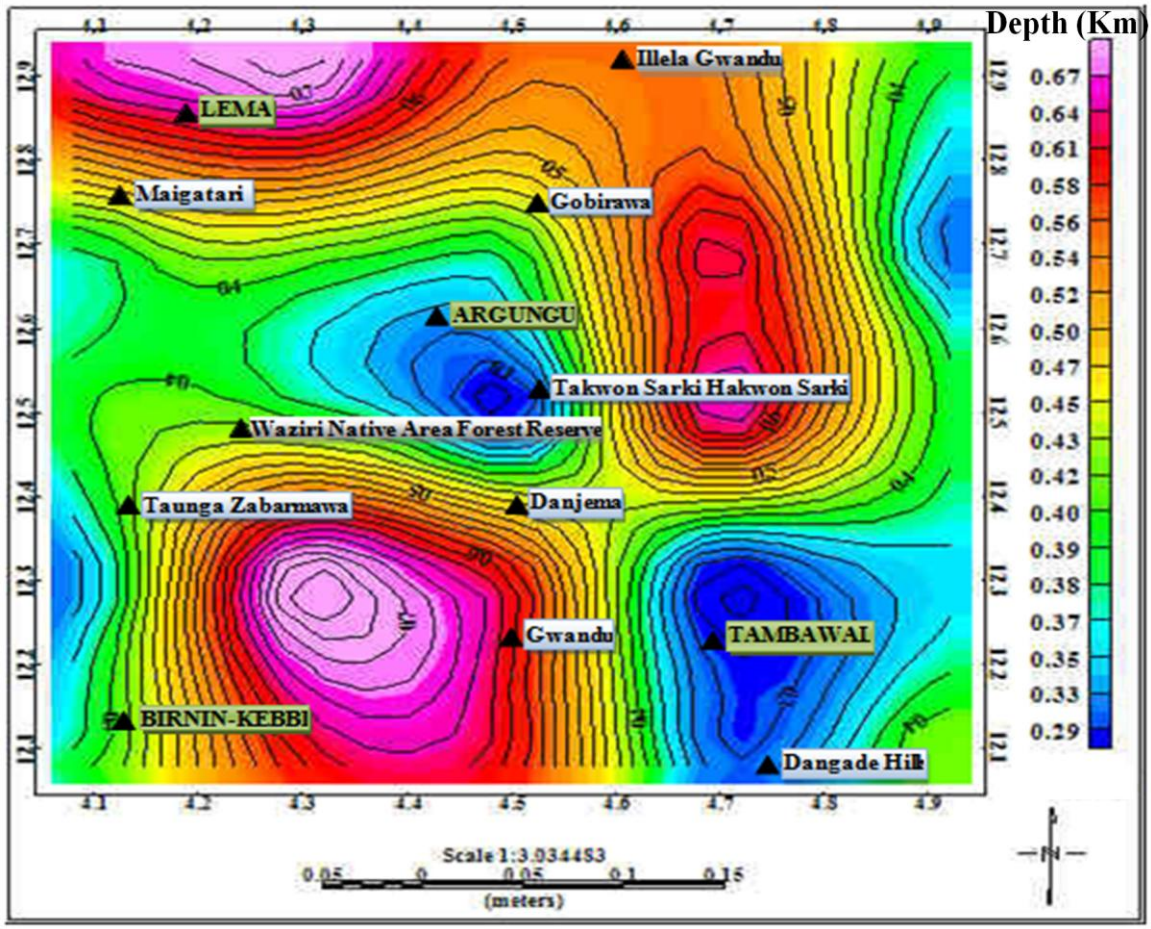

Figure 9: Depth to shallow magnetic sources (Z_1) beneath the study area

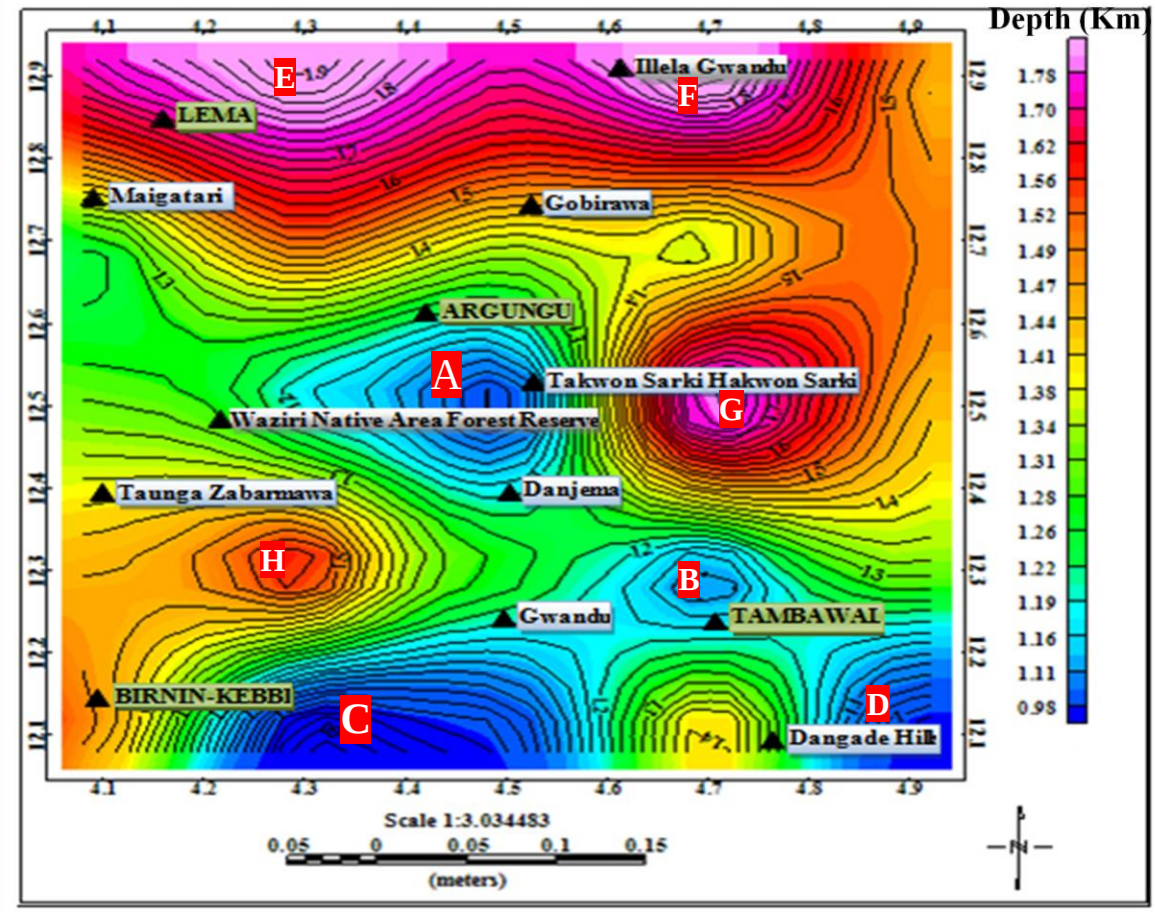

Fig. Figure 10: Depth to deeper magnetic sources (Z_2) beneath the study area.

Figure 11 shows that the depth estimates obtained using the local wave number method ranges from 0.22 km to 1.71 km, highlighting undulating basement topography beneath the area. The range of the depth estimate include those from shallow sources attributed to basement uplift and shallow intrusive/volcanic and deeper sources overlain by thick sediments. The shallow parts are generally more predominant in the south-eastern parts of the area, while deeper parts were observed to be more predominant in the northern parts around Lema, Illela Kwandu, Maigasari, Gobirawa and Argungu, in the south-western parts around Waziri area, Tunga Sabarmawa, Birnin Kebbi and Tambuwal and in the south-eastern part around Gwandu area. Further, areas associated with deeper depths are separated by shallow regions, suggesting that the deeper areas are demarcated by basement ridges, depicting horst and graben basement configuration for the area.

Comparison between Figures. 10 and 11 highlights the following correlations in the results obtained from spectral analysis and local wavenumber methods, (i) the depth range estimated from the two methods is quiet similar, (ii) undulating basement configuration typifying horst and graben structure, (iii) deepest parts of the basement around Lema, Illela Kwandu and Tunga Sabarmawa and shallow parts in the dominant portion of the south-eastern parts. Most sedimentary basins globally are known to harbour hydrocarbon and/or gas deposits, which are usually hosted in structural and/or stratigraphic traps, and produced in sub-basins/depocenters, due to thermal degradation of organic remains in potential source rocks. According to [39, 40], the minimum thickness of sediments sufficient to attain the required temperature for generation of hydrocarbons in potential source rocks ranges from 2.3 – 3.0 km. Results obtained in this study show that the maximum sedimentary thickness is below the minimum range of sedimentary thickness for commencement of hydrocarbon generation, suggesting that the area may not be viable for hydrocarbon generation.

V. CONCLUSION

Analyses of high resolution aeromagnetic data using tilt derivative, spectral analysis and local wavenumber methods were performed to delineate subsurface structures and depth to the top of magnetic sources in the area. Based on the results obtained the following conclusions were drawn from the study.

(i) The study area is underlain by linear and curvilinear structures which are oriented along different directions.

(ii) The area has been affected by different stress regimes at various stages of its evolution. The regimes were of Pan-African, Kiberan and Liberian orogenies, with the Pan- African being predominant.

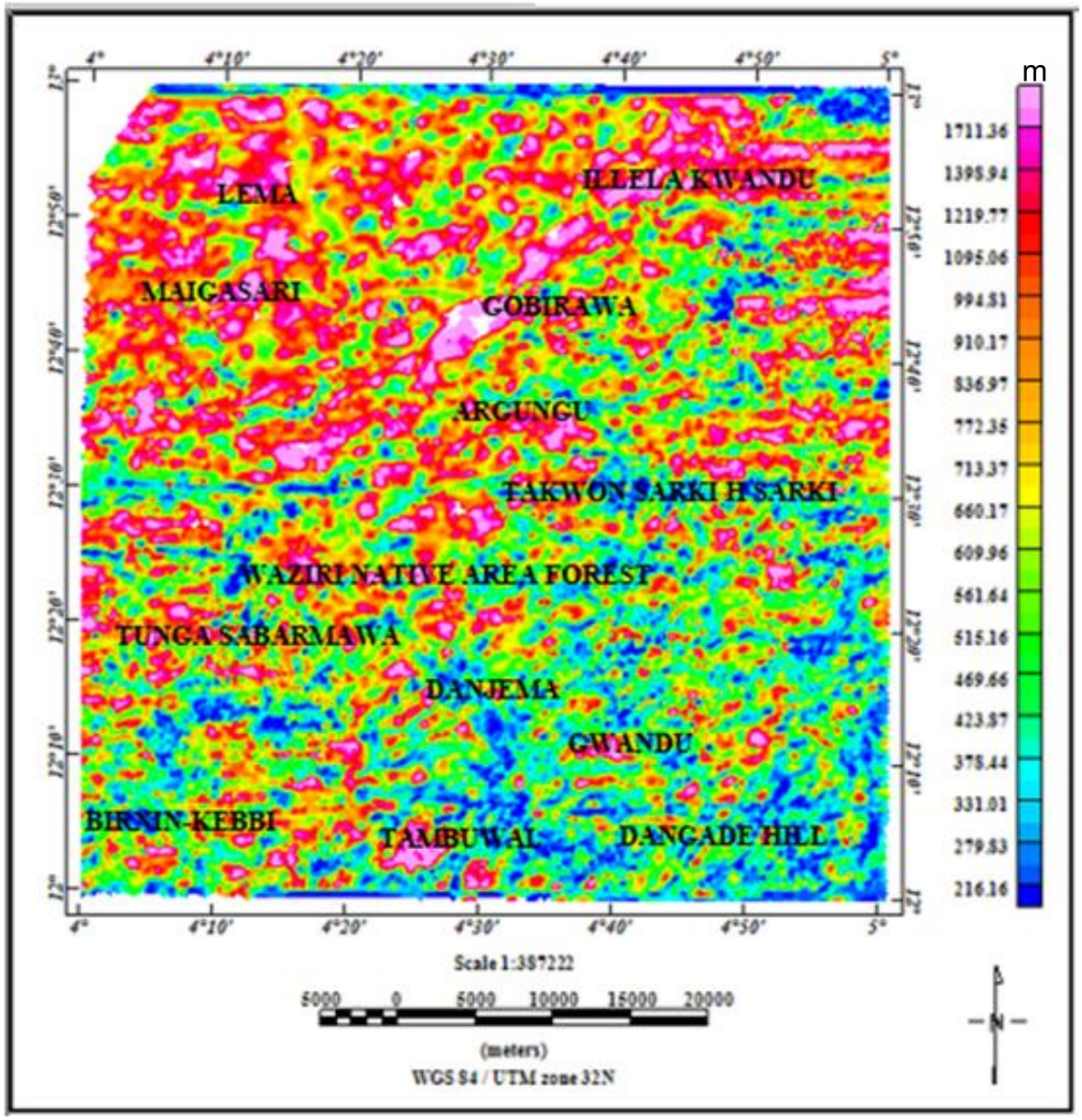

Fig 11. Local wavenumber depth estimate map of the study area.

(iii) The thickness of the sediments within the deeper parts of the area are not sufficient enough to produce hydrocarbons from the organic remains in the potential source rocks due to thermal degradation.
(iv) The deeper parts of the area are separated by basement uplifts, highlighting undulating topography typical of horst and graben basement configuration for the area.

Declaration of interest

The authors hereby declare that there is no any competing financial or personal interest that influenced the work reported in this paper.

REFERENCES

[1]. Umego, M. N., Ojo, S. B., Dyrelius, D. and Ajakaiye, D. E.. A composite magnetic anomaly map of the Sokoto basin, Northwestern Nigeria: Compilation and preliminary interpretation. *Journal of Mining and Geology*, vol 28**,** 1990, Pp309 – 315.

[2]. Shehu, A. T., Udensi, E. E., Adeniyi, J. O., Jonah, S. A.. Spectral analysis of the magnetic residual anomalies over the Upper Sokoto Basin. *Zuma Journal of Pure and Applied Science*, vol 6(2), 2004, Pp 37 – 49.

[3]. Adetona, A.A., Udensi, E. E., Agelaga, A. G. Determination of depths to buried magnetic rocks under the lower Sokoto basin. *Nigerian Journal of Physics*, vol 19(2), 2007, Pp 275 – 283.

[4]. Bonde, D. S., Udensi, E. E., Momoh, M. Modeling of magnetic anomaly zones in Sokoto Basin. *IOSR Journal of Applied Geology and Geophysics*, vol 2(1), 2014, Pp 19 - 25.

[5]. Bashar, M. G., Sanusi, Y, A. and Udensi, E. E.. Interpretation of aeromagnetic data over Birnin-Kebbi and its adjoining areas using first vertical derivative and local wavenumber methods. *IOSR Journal of Applied Geology and Geophysics*, vol 5(5), 2017, Pp 44 - 53.

[6]. Obaje, N. G. (2009). Geology and mineral resources of Nigeria.Springer, Dordrecht, pp 221.

[7]. Kogbe, C. A.. Cretaceous and Tertiary of the Iullemmedan basin of Nigeria (West Africa). *Cretaceous*,vol 2, 1981, Pp129 – 186.

[8]. Wright, J. B. D., Hasting, A., Jones, W. B. and Williams, H. R. (1985). Geology and Mineral Resources of West Africa. George Allen and Unwin, London.

[9]. Blakely,R. J. (1995). *Potential theory in gravity and magnetic applications*: Cambridge University Press. Cambridge. 441 pp

[10]. Cordell, L. L. and Grauch, V. J. S. (1985). Mapping basement magnetization zones from magnetic data from the San Juan basin, New Mexico. In Hinze, W. J. (Ed.), The Utility of Regional Gravity and Magnetic Anomaly Maps SEG: 181 – 197

[11]. Miller, H. G. and Singh, V. Potential Field Tilt: A new concept for location of potential field sources. *Journal of Applied Geophysics*, vol 32, 1994, Pp 213 – 217.

[12]. Verduzco, B., Fairhead, J. D., Green, C. M. and Mac Kenzie, C. New insights into magnetic derivatives for structural mapping. *The Leading Edge*, vol 23**,** 2004, Pp 116 – 119.

[13]. Wijins, C., Perez, C., Kowalezyk, P. Theta map: Edge detection in magnetic data. *Geophysics*, vol 70(4), 2005, Pp 39 – 43.

[14]. Pham, L. T., Okosum, E., Do, T. D., Le-Huy, M., Vu, D. M., Nguyen, V. D. LAS: A combination of the analytic signal amplitude and the generalized logistic function as a novel edge enhancement of magnetic data. *Contributions to Geophysics and Geodesy*, vol 49(4), 2019, Pp 425 – 440.

[15]. Blakely, R. J. and Simpson, R. W. (1986). Approximating edges of source bodies from magnetic or gravity anomalies. *Geophysics*, 51 (7), 2019, Pp1494 -1498.

[16]. Spector, A., Grant, F. S., 1970. Statistical models for interpretation of aeromagnetic data. *Geophysics*, **35**: 293 -302.

[17]. Hinze, W. I., Von Frese, R. B. R., Saad, A. H., 2013. Gravity and magnetic exploration, Principles, Practices and Applications. Cambridge University Press. Cambridge.

[18]. Tselentis, G., Drakopouls, J. and Dimtriads, U. A spectral approach to Moho depth estimation from gravity measurements in Epprus (NW. Greece). *Journal of Physical Earth*, vol 36, 1988, Pp255 – 266.

[19]. Thurston, J. B. And Smith, R. S. Automatic conversion of magnetic data to depth, dip, and susceptibility contrast using SPI™ method. *Geophysics*, vol 62, 1997, Pp 807 – 813.

[20]. Li, X. On the use of different methods for estimating magnetic depth. *The Leading Edge*, 22**,** 1090 – 1099.

[21]. Phillips, J. D. (2000). Locating magnetic contacts. A comparison of horizontal gradient, analytic signal and local wave number methods. 70th Annual International Meeting, SEG, Expanded abstracts: 402 - 405.

[22]. Smith, R. S., Thurston, J. B., Dai, Ting-Fan, Macleod, I. N. ISPI™ the improved source parameter imaging method. *Geophysical Prospecting*, vol 46, 1998, Pp 141 – 151.

[23]. Reynolds, J. M. (2011). An introduction to Applied and Environmental Geophysics. John Willey and Sons Ltd. Battins Line, Manchester, West Sussex, England, 696 pp.

[24]. Ngoh, J. D., Mbarga, T. N., Mickus, L., Tarek, Y., Tabod, T. C. Estimation of Curie point depth (CPD) across the Pan African Belt in northern Cameroun from aeromagnetic data. *Open Journal of Earthquake Research*, vol 9, 2020, Pp 217 – 239.

[25]. Onyedim, G. C., Alagoa, K. D., Adedokun, I. O. And Ovuru, C. Mapping high-angle basement faults in the Middle Benue Trough, Nigeria from gravity inversion surface. *Earth Science Research Journal*, vol 13(2), 2009, Pp 140 – 147.

[26]. Neev, D., Hall, J. K. And Saul, J. M. The Pelusium megesysstem across Africa and associated lineament swarms. *Journal of Geophysical Research*, vol 87, 1982, Pp 1015 – 1030.

[27]. Sanusi, Y. A. (2013). Analysis of aeromagnetic data over western parts of Nigerian Sector of the Chad basin. Unpublished PhD thesis, Abubakar Tafawa Balewa University, Bauchi, pp 168.

[28]. Avbovbo, A. A., Ayoola,, E. O., Osahon, G. A. Depositional structural styles in the Chad basin of Northeastern Nigeria. *Bulletin of American Association of Petroleum Geologists*, Vol 70, 1986, Pp 1787 – 1798.

[29]. Obiora, S. C. (2009). Field measurements in descriptions of metamorphic and igneous rocks. In Lambert- Aikhionbare, D. O. And Olayinka, A. I. (Eds)Proceedings of field mapping standardization workshop, Ibadan University Press, 105 – 125.

[30]. Tairou,, M. S., Affaton, P., Anum, S., Fleury, T. J. Pan-African paleostresses and reactivation of the Eburnean basement complex in southeast Ghana (West Africa). *Journal of Geological Research*, 2012.

[31]. Anudu, G. K., Stephenson, R. A., MacDonald, D. I. M., Oakey, G. M. Using high resolution aeromagnetic data to recognize and map intra-sedimentary volcanic rocks and geological structures across the Cretaceous Middle Benue Trough, Nigeria. *Journal of African Earth Sciences*, vol 99, 2014, Pp 625 – 636.

[32]. Genik, G.J. (1992). Regional framework, structural and petroleum aspects of rift basins in Niger, Chad and the Central African Republic (CAR). In: Zeigler, P. A. (Ed.), Geodynamics of Rifting, Vol II. Case History of Rifts: North, South America and Africa. *Tectonophysics*, **23**: 169 – 185.

[33]. Odeyemi, I. (1981). A review of the orogenic events in the Precambrian basement of Nigeria. West Africa. *Geological Rundschanu*, **70**: 897 – 909.

[34]. Ekwueme, B. N. Rb-Sr ages and petrologic features of Precambrian rocks from the Oban massif southeastern Nigeria. *Precambrian Research*, vol 47(3&4), 1990, Pp 271 - 286.

[35]. Ananaba, S. E., Ajakaiye, D. E. Evidence of tectonic control on mineralization in Nigeria from lineament density analysis: A landsat study. *International Journal of Remote Sensing*, vol 8, 1987, Pp 144-153.

[36]. Sanusi, Y. A., Muhammad, S.B. and Umego, M. N. (2019). Trend analysis of lineaments inferred from gravity data of Sokoto basin, Nigeria. 53rd annual conference, Science Association of Nigeria, UDU Sokoto, 14th – 18th July, 2019.

[37]. Labbo, Z. And Ogundoluwa, F. X. O. An interpretation of total intensity aeromagnetic maps of part of southeastern parts of Sokoto Basin. *Journal of Engineering and Applied Sciences*, vol 3, 2007, Pp 15 – 20.

[38]. Nwanko, L. I. And Shehu, A. T. Evaluation of Curie point depths, geothermal gradients and near-surface heat flow measurements from high resolution aeromagnetic data of the entire Sokoto Basin, *Nigeria. Journal of Volcanology and Geothermal Research*, vol 305, 2015, Pp 45 – 55.
[39]. Wright, J. B. D., Hasting, A., Jones, W. B. and Williams, H. R. 91985). Geology and Mineral Resources of West Africa. George Allen and Unwin, London.
[40]. Gauetier, D. L., Embry, A. M., Stoupakova, A. V., Sorensen, K. Oil and gas resource potential north of the Arctic Circle. *Petroleum Geology*, vol 35, 2011, Pp 151 – 161.